This Page Is Inserted by IFW Operations
and is not a part of the Official Record

BEST AVAILABLE IMAGES

Defective images within this document are accurate representations of the original documents submitted by the applicant.

Defects in the images may include (but are not limited to):

- BLACK BORDERS
- TEXT CUT OFF AT TOP, BOTTOM OR SIDES
- FADED TEXT
- ILLEGIBLE TEXT
- SKEWED/SLANTED IMAGES
- COLORED PHOTOS
- BLACK OR VERY BLACK AND WHITE DARK PHOTOS
- GRAY SCALE DOCUMENTS

IMAGES ARE BEST AVAILABLE COPY.

As rescanning documents *will not* correct images, please do not report the images to the Image Problem Mailbox.

II. REMARKS

Introductory Comments

Claims 21-25 were examined in the Office Action under reply and stand variously rejected under (1) 35 U.S.C. § 112, first paragraph; (2) 35 U.S.C. §102; and (3) 35 U.S.C. §103(a). These grounds of rejection are believed to be overcome by this response and are otherwise traversed for reasons discussed in detail below. Applicants note with appreciation the withdrawal of the previous rejections under 35 U.S.C. §112, second paragraph and 35 U.S.C. §102(a).

Applicants wish to thank the Examiner for the interview held on March 23, 2004 and for the helpful suggestions and comments provided at the interview. Applicants have amended the claims as discussed in the interview. Thus, all rejections are believed to be overcome.

Interview Summary

All pending rejections were discussed at the interview dated March 23, 2004. The Examiner indicated an amendment to claim 21 to eliminate the recitations regarding "therapeutic" as presented above would likely overcome the rejection under 35 U.S.C. §112, first paragraph. The Examiner also agreed to an amendment reciting that distribution is to an "area of greater than 5 mm^2," provided that applicants submit further arguments pertaining to novelty and unobviousness.

Overview of the Above Amendments

Claim 21 has been amended to recite the invention with greater particularity. Specifically, the references to a "therapeutic protein" and a "therapeutic effect" have been eliminated and claim 21 now recites that delivery is "over an area greater than 5 mm^2." As shown in Figures 1B and 3B, the range of delivery varies and can include delivery over the specified range, as well as over areas as great as 40-50 mm^2 or more, as recited in new claims 26 and 27.

The foregoing amendments are made without prejudice, without intent to abandon any originally claimed subject matter, and without intent to acquiesce in any rejection of record.

Applicant expressly reserves the right to file one or more continuing applications containing the unamended claims.

The Rejection Under 35 U.S.C. §112, First Paragraph:

Claims 21-25 remain rejected under 35 U.S.C. § 112, first paragraph, as non-enabled. The Office argues:

> The specification fails to provide adequate guidance and evidence for how to deliver a pharmaceutical composition comprising a rAAV expressing any therapeutic protein to the brain of a subject such that expression of said therapeutic protein would provide therapeutic effect for various CNS disorders in a subject via various administration routes including CED.

Office Action, page 4. Applicants maintain, for reasons of record, that the claims indeed comply with the requirements of 35 U.S.C. §112, first paragraph. Nevertheless, solely in an effort to advance prosecution, claim 21 has been amended as agreed in the interview, to delete the terminology "therapeutic." Thus, the rejection under 35 U.S.C. §112, first paragraph has been overcome and withdrawal thereof is respectfully requested.

The Rejections Over the Art:

The Office maintained the rejection of claim 21 under 35 U.S.C. §102(b) as anticipated by Okada et al., *Gene Ther.* (1996) 3:957-964 ("Okada"). The Office reiterates Okada teaches the stereotactic delivery of AAV-tk-IRES-IL-2 particles into the tumor in the brain of nude mice with a reduction in the mean volume of the tumors as compared to controls. Office Action, page 6. However, applicants disagree that Okada shows widespread distribution of rAAV virions as claimed.

All of applicants' claims require distribution of the rAAV virions **over an area greater than 5 mm^2**. Okada clearly fails to teach such distribution. Rather, Okada only demonstrates expression along the needle track. See, the abstract and page 960, column 1. Accordingly, Okada fails to anticipate the present claims and withdrawal of this basis for rejection is respectfully requested.

The Office also maintained the rejection of claims 21-24 under 35 U.S.C. §103(a) as obvious over Okada in view of PCT Publication No. WO 95/34670 to Johnson ("Johnson") and

Zhu et al., *Gene Ther.* (1996) 3:472-476 ("Zhu"). The Office argues:

> According to the collective teachings of Okada, Johnson and Zhu, it would have been obvious for one of ordinary skill at the time of the invention to deliver the AAV-tk-IRES-IL2 particles to the brain as taught by Okada via the use of osmotic minipump as taught by Zhu because they both teach delivering DNA encoding therapeutic protein, i.e. HSV-tk, into the brain of an animal to inhibit tumor growth and osmotic minipump is an administration technique for gene delivery...One having ordinary skill at the time the invention was made would have been motivated to do so in order to deliver AAV vector encoding a therapeutic protein to the brain of an animal to inhibit glioma tumor growth as taught by Okada or to treat various neurodegenerative disorder as taught by Johnson with reasonable expectation of success.

Office Action, page 8. However, applicants submit there was no reasonable expectation of success as asserted by the Office.

As explained in the interview, the fact that rAAV virions could be delivered over wide areas of the brain, such as over areas exceeding $5mm^2$, went against the conventional wisdom. Indeed, Okada, the primary reference cited by the Examiner, only showed expression along the needle track, without widespread distribution of rAAV virions. Passini et al., "Gene Delivery to the Mouse Brain with Adeno-Associated Virus" in *Methods in Molecular Biology* (Ed. W.C. Hessler), Vol. 246, pp. 225-236 ("Passini") confirm that "[a] feature of AAV2 transduction in the brain is that the vector remains confined to the injection site..." (Passini, page 225). A copy of Passini accompanies this response for the Examiner's convenience. Additionally, Vite et al., *Gene Therapy* (2003) 10:1874-1881 ("Vite") was only able to achieve distribution to areas less than 5 mm^2 using approximately two orders of magnitude more vector than applicants use. See, Table 2 of Vite, a copy of which accompanies this response.

Applicants, on the other hand, are able to achieve distribution of rAAV virions to areas ranging from at least 5 mm^2 to more than 50 mm^2! These results were completely unpredictable and unexpected given the belief in the art that rAAV distribution remained at or near the injection site. Thus, there was absolutely no expectation of success for widespread delivery of rAAV virions as claimed.

Neither of Okada or Johnson achieve distribution of rAAV virions as claimed. Both deliver AAV using stereotactic injection and as shown in Okada, such delivery only

provides for local transduction. Zhu does not pertain to viral-mediated gene delivery but rather relates to liposome-mediated gene transfer. As explained previously, rAAV virions and liposomes are completely different as liposomes are not proteinaceous and would therefore be expected to interact with a cellular membrane in a dramatically different way than AAV. Thus, there could be no expectation of success based on the teachings of Zhu. Furthermore, there is no suggestion or motivation to modify Okada and/or Johnson, using the teachings of Zhu, as asserted.

Accordingly, reconsideration and withdrawal of the rejection under 35 U.S.C. §103 is respectfully requested.

III. CONCLUSION

In view of the foregoing, applicants submit that the claims are now in condition for allowance and request early notification to that effect. If the Examiner notes any further matters which she believes may be resolved by a telephone interview, she is encouraged to contact Christina Thomson by telephone at (510)748-7208, or by fax at (510)748-7368.

Respectfully submitted,

Date: 4/15/04

By: _____
Roberta L. Robins
Registration No. 33,208

ROBINS & PASTERNAK LLP
1731 Embarcadero Road, Suite 230
Palo Alto, CA 94303
Telephone: (650) 493-3400
Facsimile: (650) 493-3440

Gene Therapy (2003) 10, 1874–1881

www.nature.com/gt

RESEARCH ARTICLE

Adeno-associated virus vector-mediated transduction in the cat brain

Charles H Vite[1,2], Marco A Passini[1,2,3], Mark E Haskins[1] and John H Wolfe[1,2]
[1]School of Veterinary Medicine, University of Pennsylvania, Philadelphia, PA, USA; and [2]Children's Hospital of Philadelphia, Philadelphia, PA, USA

Adeno-associated virus (AAV) vectors are capable of delivering a therapeutic gene to the mouse brain that can result in long-term and widespread protein production. However, the human infant brain is more than 1000 times larger than the mouse brain, which will make the treatment of global neurometabolic disorders in children more difficult. In this study, we evaluated the ability of three AAV serotypes (1,2, and 5) to transduce cells in the cat brain as a model of a large mammalian brain. The human lysosomal enzyme β-glucuronidase (GUSB) was used as a reporter gene, because it can be distinguished from feline GUSB by heat stability. The vectors were injected into the cerebral cortex, caudate nucleus, thalamus, corona radiata, internal capsule, and centrum semiovale of 8-week-old cats. The brains were evaluated for gene expression using in situ hybridization and enzyme histochemistry 10 weeks after surgery. The AAV2 vector was capable of transducing cells in the gray matter, while the AAV1 vector resulted in greater transduction of the gray matter than AAV2 as well as transduction of the white matter. AAV5 did not result in detectable transduction in the cat brain.
Gene Therapy (2003) **10**, 1874–1881. doi:10.1038/sj.gt.3302087

Keywords: *AAV; feline; animal model; central nervous system*

Introduction

A large number of single-gene disorders affect the central nervous system (CNS), many of which result from functional deficiencies of specific enzymes in metabolic pathways.[1] Somatic gene transfer has the potential to correct permanently the metabolic deficiency by transferring a normal copy of the defective gene into a patient's own cells. Gene transfer to neurons and glia of the brain requires circumvention of the blood–brain barrier, which is commonly accomplished by delivering vectors directly into the brain.[2] A major problem in treating the brain in inherited metabolic disorders is delivering the gene or its protein product globally. Although this can be achieved under certain circumstances in the mouse brain, it is a much more difficult problem in a large brain.[3–9] The brain of a child in the first year of life, when disease diagnosis is most likely and treatment is expected to be most effective, is 1000–2000 times larger than the mouse brain. To provide a foundation for initiating human gene therapy trials, gene transfer to large regions of the brain will need to be demonstrated in a large animal model.

We evaluated recombinant adeno-associated virus (rAAV) vector-mediated transduction of the cat brain following direct intracerebral inoculation. The cat was chosen for study because: (1) many naturally occurring inherited metabolic disorders affect the cat brain;[10–12] (2) the feline nervous system has been well-characterized both anatomically and physiologically;[13,14] (3) the cat brain is approximately 100 times larger than the mouse brain, and (4) the physical organization of the cat brain is more similar to the human brain than is the rodent brain.

Recombinant AAV vectors are excellent for gene transfer to the CNS. They are nonpathogenic, can be produced in high titers, can infect the nondividing cells of the brain, and can result in long-term gene expression in the murine brain.[15] Nine AAV serotypes have been identified, which differ in their capsids proteins.[15,16] Comparison of the ability of three different AAV serotypes, AAV2, 4, and 5, to transduce the mouse brain revealed that while intrastriatal injection of either AAV2 or AAV5 led to transgene-positive parenchymal cells, AAV5 resulted in the greatest number of transgene-positive cells.[17] We compared the ability of three rAAV serotypes, AAV1, 2, and 5, to achieve gene transfer in the normal cat brain. β-glucuronidase (GUSB) was used as a marker gene due to the ability to monitor enzyme expression using histochemical staining and mRNA expression using *in situ* hybridization on frozen brain sections.

Results

A plasmid containing AAV2 inverted terminal repeats (ITRs) flanking a transcription unit (HβH) containing the human GUSB cDNA under the control of the human GUSB promoter was cross-packaged into AAV1, AAV2,

Correspondence: Dr JH Wolfe, 502 Abramson Research Center, Children's Hospital of Philadelphia, 3516 Civic Center Blvd., Philadelphia, PA 19104-4318, USA
[3]*Current address: Genzyme Corporation, Framingham, MA, USA*
Received 28 January 2003; accepted 22 April 2003

	AAV 2/1	AAV 2/2	AAV 2/5	Uninjected
Cat #1	Left	Right		
Cat #2	Left	Right		
Cat #3	Left		Right	
Cat #4		Left	Right	
Cat #5		Left	Right	
Cat #6				U
Cat #7				U

Figure 1 Injection sites in the cat brain. A dorso-ventral view of the cat brain is shown. The four injection sites in the right cerebral hemisphere are identified by Xs. A Hamilton syringe and needle were used to deliver each serotype to the brain. Each dorso-ventral injection track passed through at least one of the brain structures of interest. Transduction of the frontal cortex and corona radiata was assessed at site 1; transduction of the caudate nucleus was assessed at site 2; transduction of the thalamus was assessed at site 3; transduction of the centrum semiovale and the internal capsule were assessed at site 4. Each of five cats was injected with two of the three AAV serotypes. Each cerebral hemisphere (left or right) received only one serotype. No cats received the same serotype in both cerebral hemispheres. Cats 6 and 7 were not injected with a vector (UI=uninjected).

and AAV5 capsids, resulting in three viral vectors each containing the same recombinant genome. The titer of each of the three viral vectors, designated AAV2/1, AAV2/2, and AAV2/5, was 4.9×10^{12}, 4.5×10^{12}, and 4.5×10^{12} genomic equivalents (GE)/ml, respectively.

Eight-week-old cats (n=5) were injected intracerebrally with AAV vectors (Figure 1). Cats were injected with a total of 50 µl (~12 µl per needle track) of either the AAV2/1, AAV2/2, or AAV2/5 vector. Each injected hemisphere received only one AAV serotype and no cats received the same serotype in both cerebral hemispheres. All cats recovered and were eating well within 12 h of surgery. No cats showed any abnormal clinical signs during the 10-week period of study.

Expression of GUSB activity in the brain

The five injected cats were euthanized 10 weeks after surgery (18 weeks of age) along with two uninjected, age-matched control cats. The brains were perfused, removed, formalin-fixed, frozen, sectioned transversely, and examined for GUSB activity using a histochemical stain.[18] Low levels of endogenous intracellular feline GUSB activity were undetectable with this method, although the white matter stained diffusely a pale pink (not shown). This faint staining was removed by heating slides to 65°C prior to staining to inactivate native feline GUSB in the same manner used to inactivate murine GUSB compared to human GUSB, which is heat stabile.[8,19] A mild to moderate infiltration of inflammatory cells was variably seen along the needle track in all injected cats.

Injection of AAV2/1 and AAV2/2 resulted in detectable GUSB activity, as assessed by histochemical staining, along the needle track in the gray matter (cortex of the frontal lobe, the caudate nucleus, and the thalamus) (Figure 2a, b, d, e, g, h). Cats injected with AAV2/5 (Figure 2c, f, i) and uninjected control cats (Figure 2j) showed no histochemical evidence of GUSB activity in the gray matter. Comparison of AAV2/1 *versus* AAV2/2 in the gray matter showed qualitatively stronger histochemical staining and positively stained cells at farther distances from the needle track with AAV2/1. AAV2/2 resulted in most cells staining positive for GUSB activity immediately adjacent to the needle track (Figure 2b, e, h). In contrast, AAV2/1 resulted in many GUSB-positive cells as far as 2 mm from either side of the needle track (Figure 2a, d, g). The histochemical staining in AAV2/1-injected cats was the strongest in the caudate nucleus (Figure 2d). Similar patterns of GUSB activity were found in all three cats injected with AAV2/1 and AAV2/2.

The maximum rostro-caudal and medio-lateral distances from the needle track in which GUSB-positive cells were present in the gray matter was measured in cats injected with the same vector, averaged, and compared between AAV2/1- and AAV2/2-injected cats (Table 1). The diameter of the region of brain surrounding the needle track that contained GUSB-positive cells was significantly greater ($P<0.05$) in AAV2/1-injected cats than in AAV2/2-injected cats in the caudate nucleus (Table 1). A second quantitative method was also used to compare GUSB staining between cats injected with different vectors. On the brain section containing the needle track, the area of GUSB-positive brain was calculated and compared between AAV2/1 and AAV2/2 (Figure 3; Table 2). AAV2/1 resulted in a significantly greater area of GUSB-positive cells in the caudate nucleus than did AAV2/2.

In contrast to the gray matter, only AAV2/1 produced significant GUSB activity in the white matter (corona radiata of the frontal lobe, the centrum semiovale, corpus callosum, and the internal capsule) (Figure 4a, d, h). GUSB-positive cells in AAV2/1-injected brains were found up to 5 mm from the needle track. In all cases, GUSB-positive cells were distributed along the white matter tracts and the number of positive cells diminished at increasing distances from the needle track (Figure 4a, d, h). Injection of AAV2/2 only resulted in rare GUSB-positive cells in the centrum semiovale and internal capsule (Figure 4e,i). Interestingly, the gray matter both dorsal and ventral to the white matter tract often showed many GUSB-positive cells after AAV2/2 injection (4i).

Finally, in AAV2/1-injected cats, GUSB-positive cells could be found in a continuous line in the injection tracks extending from the dorsal cortex, through the corona radiata, the deep gray matter (caudate nucleus or thalamus), the internal capsule, to the ventral cortex (a dorso-ventral distance of 25 mm).

In situ hybridization

Since GUSB is a secreted enzyme that is endocytosed by neighboring untransduced cells,[20,21] we determined whether histochemically positive cells were cross-corrected or whether they expressed GUSB mRNA. In all

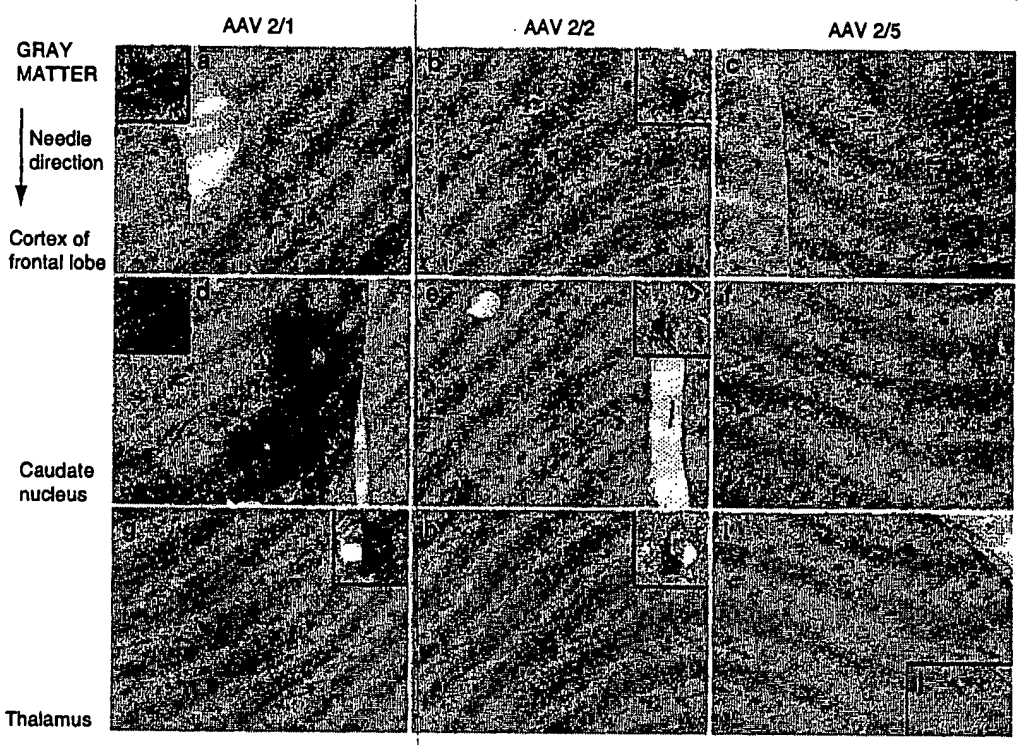

Figure 2 GUSB histochemistry in the gray matter. Comparison of AAV2/1, AAV2/2, and AAV2/5 vectors' ability to transfer GUSB activity to the cerebral cortex, caudate nucleus, and thalamus showed that both AAV2/1 (a,d,g) and AAV2/2 (b,e,h) transferred GUSB activity to these gray matter structures. Qualitative comparison of AAV2/1 and AAV2/2 showed that AAV2/1 transferred GUSB activity to a larger area than AAV2/2. Neither the AAV2/5-injected cat brain (c,f,i) nor the uninjected control cat brain (j) showed any evidence of GUSB activity. (lettered panels= × 25 magnification; insets= × 400 magnification; size bar in panel c=0.5 mm).

Table 1 Comparison of the average maximum distance (mm) in which GUSB-positive cells were present in the gray matter between AAV2/1- and AAV2/2-injected cats

	AAV2/1	*AAV2/2*
Gray matter		
Cerebral cortex		
Rostro-caudal diameter (mm)	1.71±0.50	1.32±0.12
Medio-lateral diameter (mm)	1.72±0.44	1.92±0.18
Caudate nucleus		
Rostro-caudal diameter (mm)	3.22±0.63*	0.82±0.31
Medio-lateral diameter (mm)	2.88±0.70*	1.20±0.71
Thalamus		
Rostro-caudal diameter (mm)	2.75±0.55	2.24±0.57
Medio-lateral diameter (mm)	2.70±0.68	2.68±0.71
White matter		
Corona radiata		
Rostro-caudal diameter (mm)	1.59±0.64	UM
Medio-lateral diameter (mm)	1.67±0.42	UM
Internal capsule		
Rostro-caudal diameter (mm)	2.94±0.51	UM
Medio-lateral diameter (mm)	2.40±0.88	UM
Centrum semiovale		
Rostro-caudal diameter (mm)	2.69±0.65	UM
Medio-lateral diameter (mm)	4.04±1.03	UM

In the caudate nucleus, AAV2/1 resulted in GUSB-positive cells at significantly greater distances from the needle tract compared to AAV2/2 (*$P<0.05$). Only AAV2/1 transferred significant GUSB activity to the white matter (UM=unmeasureable).

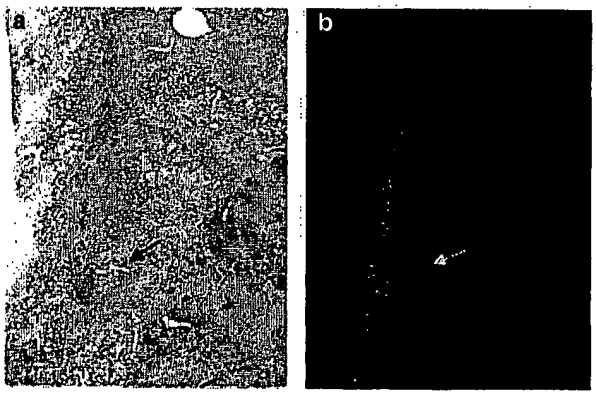

Figure 3 Measurement of area of GUSB-positive brain regions. Panel (a) shows the normal appearance of a brain section at the level of the caudate nucleus at × 25. Note the vertical line of GUSB-positive cells to the left of the image (arrows). Using a software program, the region of GUSB-positive staining was accentuated from the background (panel b). The area of this region was then calculated in each injected cat.

brain regions where AAV2/1 or AAV2/2 produced GUSB-positive cells as assessed by histochemistry, cells were identified that were positive for GUSB mRNA expression by *in situ* hybridization (Figure 5). When individual regions were compared, there was direct overlap of *in situ* hybridization-positive cells with GUSB-

positive cells (Figure 6). No *in situ* hybridization-positive cells were found in the brains of cats injected with AAV2/5 or in uninjected cats.

Discussion

Nine AAV serotypes have been identified.[16,22–26] Specific AAV serotypes differ in the composition of their capsid proteins and in their ability to transduce lung, muscle, and brain.[27] Cross-packaging of the AAV2 vector genome into other AAV serotypes demonstrated that the amino acids of the capsids are responsible for some of the differences in cellular tropism.[16,17,26,28,29] The different capsids likely result in differences in binding to cellular receptors as evidenced by the ability of AAV1, AAV2, and AAV3 to bind to heparan sulfate, while AAV4 and 5 do not.[25,27] The receptors for AAV2 and AAV5, heparan sulfate proteoglycans and 2,3-linked sialic acid, respectively, have been determined.[27,30] The cellular receptor for AAV1 has not been identified.

In the mouse brain, gene transfer using three recombinant AAV serotypes, AAV2, AAV4, and AAV5, with a variety of promoters and genes has been performed.[3–5,7,8,17,31–34] All but two studies examined AAV2-mediated transduction alone.[17,35] A direct comparison of intracerebral injection in adult mice of AAV2, AAV4, and AAV5, each containing the Rous sarcoma virus (RSV) long-terminal repeat promoter and the lacZ gene, found that AAV2 and AAV5 could transduce cells in the striatum, but that AAV5 resulted in greater numbers of positive cells at longer time points, whereas, AAV4 resulted in almost exclusive transduction of ependymal cells.[17] In this study, the AAV2 and AAV4 vectors each contained the same vector genome and differences in transduction patterns could only be explained by differences in the composition of the viral capsids. In contrast, the AAV5 vector used the AAV5 inverted terminal repeats (ITRs), which may have contributed to the differences in gene expression.[17]

Three other species (rat, gerbil, and monkey) have been examined for AAV vector transduction in the brain. However, since a variety of promoters, transgenes, ITRs, and brain regions have been used, a direct comparison between species is not possible.[36–41] A comparison of AAV2 and AAV5 injection into the rat striatum indicated that AAV5 transduction was less predictable in the direction of spread and in the volume of transduction than AAV2.[41] There have been no studies examining the ability of AAV1 to transduce the brain in the adult of any species.

Table 2 Comparison of the average transverse area (mm^2) in which GUSB-positive cells were present in the gray matter of AAV2/1- and AAV2/2-injected cats

	AAV2/1	*AAV2/2*
Gray matter		
Cerebral cortex	1.13±0.38	1.12±0.63
Caudate nucleus	4.27±0.55*	0.59±0.12
Thalamus	1.63±0.71	1.06±0.02
White matter		
Corona radiata	1.65±0.85	UM
Internal capsule	2.92±1.17	UM
Centrum semiovale	4.59±0.94	UM

In the caudate nucleus, AAV2/1 resulted in a significantly greater area of GUSB positive cells compared to AAV2/2 (*$P<0.05$). Only AAV2/1 transferred significant GUSB activity to the white matter (UM=unmeasureable).

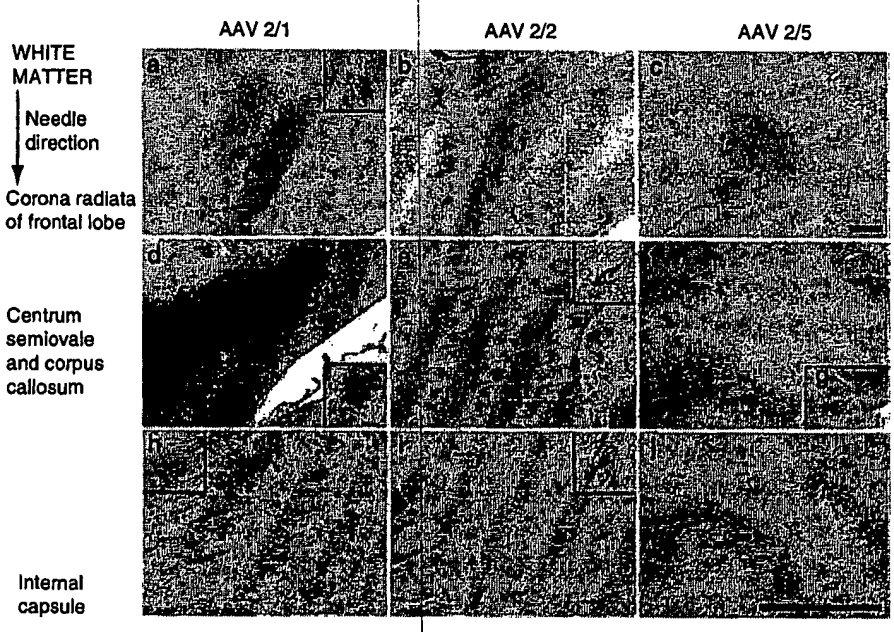

Figure 4 GUSB activity in the white matter. AAV2/1 transferred GUSB activity to the corona radiata, centrum semiovale, corpus callosum, and internal capsule (a,d,h). In contrast, AAV2/2-injected cat brain showed rare GUSB-positive cells within the white matter (arrowheads in e and i) and evidence of transduction of gray matter surrounding the white matter (arrows in i). Neither the AAV2/5-injected cat brain (c,f,j) nor the uninjected control cat brain (g) showed any evidence of GUSB activity. (lettered panels a–f= ×25 magnification; lettered panels h–j= ×100 magnification; insets= ×400 magnification; size bar in c and j=0.5 mm).

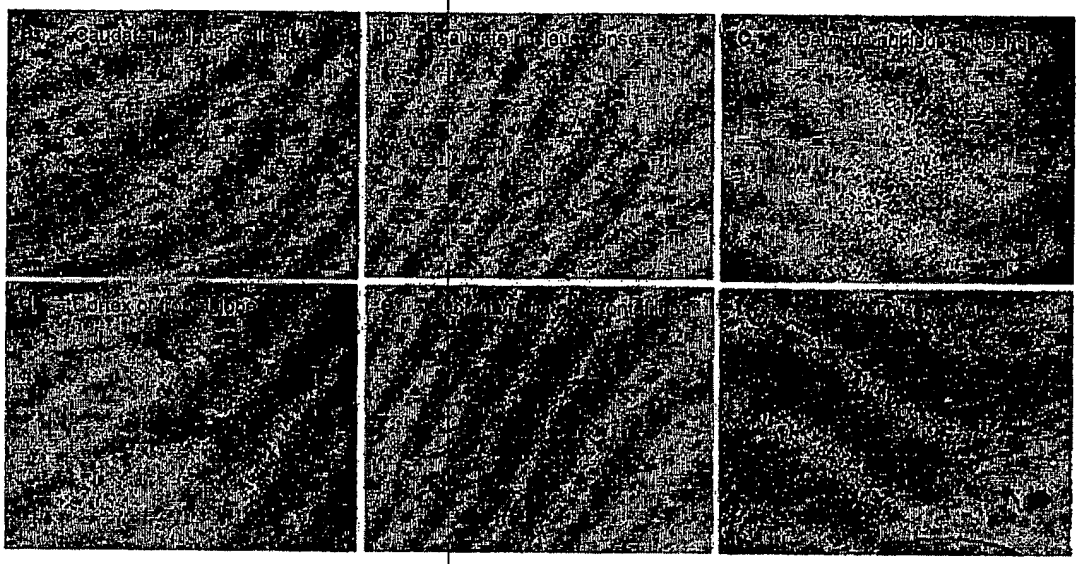

Figure 5 In situ hybridization for GUSB mRNA. In situ hybridization results shown are for brains injected with AAV2/1. Panels (c–f) show significant in situ hybridization in brain sections hybridized to the antisense riboprobe. These results show that in all brain regions where histochemistry showed GUSB-positive cells (Figures 2 and 4), in situ positive cells were found. Panel (a) shows no staining in a brain section where no probe was used in the protocol. Panel (b) shows very mild staining in the brain section where sense riboprobe was used.

Figure 6 In situ hybridization for GUSB mRNA in AAV2/1-infected brains. Both histochemistry (panel a) and in situ hybridization (panel b) demonstrate transduction of the caudate nucleus (CN), thalamus (TH), and internal capsule (IC) in this cat brain injected with AAV2/1. The regions of in situ positive and GUSB-positive cells overlapped in all brain regions examined.

For studies in the cat brain, each of the three vectors contained the same genome with the only difference being the composition of the capsids. Of the three serotypes tested, only AAV2/1 and AAV2/2 were capable of transducing the cat brain as determined by *in situ* hybridization. Low levels of *in situ* hybridization positive staining were seen with the sense riboprobe. We have also observed this in mice where it has been shown that episomal forms of vector DNA persist in brain tissue, therefore, small amounts of sense riboprobe may have hybridized to the nontranscribed strand of the episomal DNA.[3,42] No evidence of hybridization was seen in regions of uninjected brain using either the sense or antisense riboprobe.

In all cats, positive histochemical staining colocalized with positive *in situ* hybridization staining. This indicated the presence of vector genome in the majority of histochemically positive cells and only local spread of enzyme by diffusion between cells. However, the distal spread of enzyme activity away from transduced cells may be below histochemical detection.[21] No evidence of retro- or anterograde transport in the cat brain was found with any of the three serotypes used. Although axonal transport of a lysosomal enzyme has been reported in the mouse,[42] there are several possible explanations for this apparent difference. First, the regions of the brain in which transport was examined in the mouse, the intrahippocampal and septohippocampal pathways, were not tested in the cat so a direct comparison is not possible. Second, substantial evidence of axonal transport in the mouse brain was not identified until 12 weeks post-transduction in the mouse. Since the cat brain is significantly larger than the mouse brain, with correspondingly longer axons, it is possible that evidence of axonal transport would not be found until much later than 10 weeks after viral injection. Third, low levels of enzyme may have undergone axonal transport, but were below the limits of histochemical detection. Finally, although possible, it seems unlikely that differences in axonal transport of lysosomal enzymes would exist between species.

Comparison of AAV2/1 to AAV2/2 showed that while both were capable of transducing cortical and deep gray matter of the brain, AAV2/1 transduced a larger region of brain and at farther distances from the injection track, particularly in the caudate nucleus. In contrast, only AAV2/1 was capable of transduction of the white matter. These data suggest that while the receptors for both AAV1 and AAV2 are present within the gray matter of the cat brain, only AAV1 receptors are found in the white matter. In the mouse brain, AAV2 transduces primarily neurons.[3,8,17,42,43] In the cat brain, the fact that AAV2/2 transduces only the gray matter, in addition to the neuronal-like shape of the transduced cells (Figure 2), suggests that neuronal transduction is also occurring. In the cat, AAV2/1 transduced both gray and white matter in the cat brain, suggesting that AAV2/1 is capable of also

transducing oligodendrocytes. Similar patterns of gray and white matter transduction have been found in the adult mouse brain (MAP and JHW, unpublished). Unfortunately, an antibody capable of selectively identifying oligodendrocytes is not available for use in cats and these studies will need to be performed in the rodent model.

Injection of AAV2/5 did not result in detectable transduction in the cat brain. In contrast, AAV5 resulted in significant transduction of the mouse brain but, in those experiments, an expression cassette flanked by AAV5 ITRs was used.[17,35] In the cat experiments, the expression cassette was flanked by AAV2 ITRs and a eucaryotic promoter was used. Since the promoter, cDNA, ITR, and viral titer may all effect transduction,[15] it is not known whether differences in transduction between the mouse and cat were due to species or vector differences. We are currently examining the transduction pattern of different AAV serotypes in the mouse brain. The same viral preparation of AAV2/5 resulted in transduction of the choroid plexus and ependymal cells of the mouse brain (MAP and JHW, unpublished). It will be important to compare transduction patterns among species and it must be noted that the transduction pattern seen in the cat and mouse may differ in primates.

There is a wealth of basic data on the cat brain due to the decades-long use of cats in neurobiological studies.[13,14] There are also many single-gene disorders in the cat that affect the CNS, making the cat a useful model for diseases that affect human patients.[10–12] Our studies show that AAV2/1 was the most efficient at transferring GUSB activity in major gray and white matter structures of the cat brain. Indeed, AAV2/1 transduced all regions along the dorso-ventral needle track resulting in a vertical 'cylinder' of transduction. Using an averaged 1.5 mm radius of transduction from the injection track results in a calculated 7.1 mm^2 dorsal-plane cross-sectional area of transduction around each needle track.

The data from these experiments are being used to design treatment strategies for diffuse brain disease, such as lysosomal storage diseases, which occur naturally in the cat. One of these diseases, mucopolysaccharidosis type VII (MPSVII), is caused by inherited GUSB deficiency that results in the lysosomal storage of substrate. In MPS VII and other lysosomal storage diseases, correction of mutant cells by direct gene transfer results in correction of storage in the transduced cell as well as in neighboring untransduced cells. Correction of storage in neighboring cells occurs by endocytosis of secreted lysosomal enzymes from transduced cells.[20,21] Our studies in the MPSVII mouse have shown that the secreted GUSB can resolve lysosomal storage lesion in the brain at least 2 mm away from GUSB positively stained cells.[3,21] This shows that although enzyme was present in neighboring untransduced cells, it was below the level of histochemical detection. Using AAV2/1 in the cat brain, if GUSB were present at therapeutic levels 2 mm beyond histochemically positive areas, this would result in an approximately 38 mm^2 dorsal-plane cross-sectional area of correction. Thus, the whole cat brain, which at its widest dorsal-plane width is approximately 1250 mm^3, could be corrected by approximately 33 injection tracks. Assuming similar transduction and enzyme secretion in the human infant brain and a dorsal-plane cross-sectional area of 14 000 mm^2, approximately 368 injections would be necessary for correction. The use of stronger promoters to increase the total amount of GUSB secreted from transduced cells could reduce the total number of injections needed by further extending the radius of correction.

Methods

rAAV vector production

The detailed construction of the rAAV genome used in this study was previously reported.[8] The genome contained AAV2 ITRs flanking a 2.6 kb transcription unit (HβH) containing the human 2.2 kb GUSB cDNA under the control of the 0.4 kb human GUSB promoter, a 0.4 kb SV40 splice donor–acceptor and poly A sequences, and a 1.4 kb stuffer sequence that resulted in a genome size of 4.7 kb. The plasmid was cross-packaged, by the Institute of Human Gene Therapy at the University of Pennsylvania, into AAV1, AAV2, and AAV5 capsids resulting in three viral vectors each containing the same AAV2-HβH genome.[26,44] The titer of each of the three viral vectors, designated AAV2/1, AAV2/2, and AAV2/5, was 4.9×10^{12}, 4.5×10^{12}, and 4.5×10^{12} GE/ml, respectively.

Animals

Seven normal cats were raised in the animal colony of the School of Veterinary Medicine of the University of Pennsylvania, under NIH and USDA guidelines for the care and use of animals in research. The animals were housed at 21°C with *ad libitum* food and water, 12-h light cycles, with 12–15 air changes per hour. At 8 weeks of age, five cats were anesthetized with intravenous propofol (up to 6 mg/kg; Abbott Laboratories, Chicago, IL, USA), endotracheally intubated, maintained under anesthesia with isoflurane (IsoVet; Schering-Plough, Omaha, NE, USA), and placed in a nonferrous stereotaxic head holder designed by the investigators. The brain was imaged either by computerized tomography or magnetic resonance imaging to determine the coordinates of the brain structures of interest. These included the cortex of the frontal lobe, the head of the caudate nucleus, the thalamus, the corona radiata of the frontal lobe, the centrum semiovale, and the internal capsule. Following imaging, each cat was prepared for surgery. A midline incision was made over the dorsum of the calvaria and four holes, 1 mm in diameter, were drilled in each side of the calvaria over the brain regions of interest (Figure 1). A 25 µl Hamilton syringe with a 26 G needle was used to administer each rAAV vector. The needle was placed into each drill hole and lowered to the base of the brain, 2 µl of vector was injected and allowed for vector diffusion for 2 min. The needle was then withdrawn vertically at 0.5 cm distances and the injection procedure repeated until the needle was no longer in the brain. A total of 50 µl of vector was administered per cerebral hemisphere of each cat. Each cerebral hemisphere received only one of the rAAV serotypes (Table 1). The two additional cats served as control cats for *in situ* hybridization and histochemistry and did not have surgery performed.

Preparation of brain tissue

The five injected cats were killed at 18 weeks of age, 10 weeks after surgery, using an intravenous overdose of

barbiturate (Fatal-Plus; Vortech Pharmaceuticals, Dearborn, IL, USA) in accordance with the American Veterinary Medical Association guidelines. Additionally, two uninjected cats were killed at 18 weeks of age. Immediately prior to killing 0.5 cc of heparin (1000 U/ml) was administered intravenously. Following killing, intracardiac perfusion with 250 ml of 0.9% cold saline was followed by 750 ml of neutral buffered 10% formalin containing 0.75 g chloral hydrate. Brains were removed, sectioned transversely, fixed in 10% formalin/chloral hydrate for an additional 24 h and then transferred to 30% sucrose–phosphate-buffered saline at 4°C until the sections no longer floated. Brain sections were then placed in OCT media (Tissue-Tek; Sakura Finetechnical Co, Tokyo, Japan), frozen, and cryosectioned transversely at a thickness of 20 μm. Tissue sections were placed on slides for staining and stored at −20°C until staining was performed.

Enzyme histochemistry

GUSB activity was assessed in frozen tissue by staining with a naphthol-AS-BI-β-D-glucuronide substrate and a pararosaniline dye that stains tissue red when GUSB activity is present.[18] Low levels of endogenous intracellular feline GUSB activity were undetectable with this method, although the white matter stained diffusely a pale pink. This faint staining was removed by heating slides to 65°C prior to staining to inactivate native feline GUSB in the same manner used to inactivate murine GUSB.[8,19] The human GUSB was not heat labile resulting in positive histochemical staining in the brains of transduced cats.

The distance from the needle track and the area in which red, histochemically positive cells were present was measured using a microscope and a software program (ImagePro Plus; Media Cybernetics LP, Silver Springs, MD, USA).[45] Several brain sections were stained for GUSB activity and to locate hemosiderin that was used to identify the injection site. When hemosiderin was identified, the rostro-caudal distance of GUSB-positive cells was measured from this site by staining sections every 100 μm until the limit of GUSB-positive cells was reached. The medio-lateral limit was measured in each brain at the level of the injection track; measurements were made on two slides per each injection track. Area measurements were made on the histologic section containing the needle track, as evidenced by the presence of a visible linear line of hemosiderin resulting from the needle insertion. Area measurements were made on two slides per each injection track. The area in which GUSB-positive cells were present was measured by capturing digital bright field images, subtracting the green channel from the red channel and measuring the area of red staining on each slide. Subtraction of the green channel was performed to accentuate the red-stained area, because in unstained regions the intensities of the green and red images are similar but in stained regions there is an increased absorption of green light passing through the stain.

In situ hybridization

Nonradioactive *in situ* hybridization was performed on frozen tissue sections to detect hGUSB mRNA. A 1590 bp segment of the hGUSB cDNA was cloned into the Bluescript (Stratagene, La Jolla, CA, USA) plasmid. The plasmid was linearized to generate antisense and sense templates for runoff transcription from the *cis*-acting viral promoters. Digoxigenin-labeled (Roche, Indianapolis, IN, USA) antisense and sense cRNA probes were generated and the probe length was verified on a formaldehyde gel. The *in situ* hybridization protocol and colorometric staining using an alkaline phosphatase-mediated BCIP/NBT reaction has been previously described.[8,46] Sections from both *in situ* hybridization and enzyme histochemistry reactions were mounted on 100% glycerol and photographed using a light microscope (Carl Zeiss Axioplan, Germany).

Statistics

Mean and standard deviation were used for comparison of all data. The unpaired *t*-test was used to compare distance from the needle track and area containing GUSB-positive cells between AAV2/1 and AAV2/2. Significance was determined when $P<0.05$.

Acknowledgements

CHV was supported by a K08 from NINDS (NS02032) and MAP by an NIH training grant (DK07748). We thank P O'Donnell, J Zweigel, and T O'Malley and the Animal Models Core of the School of Veterinary Medicine (RR02512) for assistance with the animal procedures; AC Polesky and B Chambers for assistance in sectioning and processing tissue; M Parente for assistance in image analysis; and L Wang and the Vector Core of the University of Pennsylvania (DK47747) for assistance in viral vector production. This work was supported in part by NIH Grants NS38690, DK63973, and DK49652.

References

1 Scriver CR, Beaudet AL, Sly WS, Valle D. *Metabolic Bases of Inherited Disease* 8th edn. McGraw Hill: NY, 2001, pp 3369–3894.
2 Sly WS, Vogler C. Brain-directed gene therapy for lysosomal storage disease: going well-beyond the blood–brain barrier. *Proc Natl Acad Sci USA* 2002; 99: 5760–5762.
3 Skorupa AF *et al.* Sustained production of β-glucuronidase from localized sites after AAV vector gene transfer results in widespread distribution of enzyme and reversal of lysosomal storage lesions in a large volume of brain in mucopolysaccharidosis VII mice. *Exp Neurol* 1999; 160: 17–27.
4 Daly TM *et al.* Neonatal gene transfer leads to widespread correction of pathology in a murine model of lysosomal storage disease. *Proc Natl Acad Sci USA* 1999; 96: 2296–2300.
5 Elliger SS *et al.* Elimination of lysosomal storage in brains of MPS VII mice treated by intrathecal administration of an adeno-associated virus vector. *Gene Therapy* 1999; 6: 1175–1178.
6 Ghodsi A *et al.* Systemic hyperosmolality improves β-glucuronidase distribution and pathology in murine MPS VII brain following intraventricular gene transfer. *Exp Neurol* 1999; 160: 109–116.
7 Bosch A *et al.* Reversal of pathology in the entire brain of mucopolysaccharidosis type VII mice after lentivirus-mediated gene transfer. *Hum Gen Ther* 2000; 11: 1139–1150.
8 Passini MA, Wolfe JH. Widespread gene delivery and structure specific patterns of expression in the brain after intraventricular injections of neonatal mice with an adeno-associated virus vector. *J Virol* 2001; 75: 12382–12392.

9 Brooks AI *et al*. Functional correction of established central nervous system deficits in an animal model of lysosomal storage disease with feline immunodeficiency virus-based vectors. *Proc Natl Acad Sci USA* 2002; 99: 6216–6221.
10 Summers BA, Cummings JF, de Lahunta A. *Veterinary Neuropathology*., Mosby: St Louis, MO, 1995.
11 Jolly RD, Walkley SU. Lysosomal storage diseases of animals: an essay in comparative pathology. *Vet Pathol* 1997; 34: 527–548.
12 Watson DJ, Wolfe JH. Lentiviral vectors for gene transfer to the central nervous system: applications in lysosomal storage disease animal models. In: Machida C (ed). *Viral Vectors for Gene Therapy: Methods and Protocols*, Humana Press: Totowa, NJ, 2002 pp 383–403.
13 Berman AL. *The Brain Stem Of The Cat, A Cytoarchitectonic Atlas With Stereotaxic Coordinates*, University of Wisconsin Press: Madison, 1968.
14 Berman AL, Jones EG. *The Thalamus And Basal Telencephalon of the Cat: A Cytoarchitectonic Atlas with Stereotaxic Coordinates*, University of Wisconsin Press: Madison, 1982.
15 Rabinowitz JE, Samulski RJ. Building a better vector: the manipulation of AAV virions. *Virology* 2000; 278: 301–308.
16 Gao G-P *et al*. Novel adeno-associated viruses for rhesus monkeys as vectors for human gene delivery. *Proc Natl Acad Sci USA* 2002; 99: 11854–11859.
17 Davidson BL *et al*. Recombinant adeno-associated virus type 2, 4, and 5 vectors: transduction of variant cell types and regions of the mammalian central nervous system. *Proc Natl Acad Sci USA* 2000; 97: 3428–3432.
18 Wolfe JH, Deshmane SL, Fraser NW. Herpesvirus vector gene transfer and expression of β-glucuronidase in the central nervous system of MPS VII mice. *Nat Genet* 1992; 1: 379–384.
19 Casal ML, Wolfe JH. *In utero* transplantation of fetal liver cells in the mucopolysaccharidosis type VII mouse results in low-level chimerism, but overexpression of beta-glucuronidase can delay onset of clinical signs. *Blood* 2001; 97: 1625–1634.
20 Fratantoni JC, Hall CW, Neufeld EF. Hurler and Hunter syndromes: mutual correction of the defect in cultured fibroblasts. *Science* 1968; 162: 570–572.
21 Taylor RM, Wolfe JH. Decreased lysosomal storage in the adult MPS VII mouse brain in the vicinity of grafts of retroviral vector-corrected fibroblasts secreting high levels of β-glucuronidase. *Nat Med* 1997; 3: 771–774.
22 Chirioni JA *et al*. Cloning of adeno-associated virus type 4 (AAV4) and generation of recombinant AAV4 particles. *J Virol* 1997; 71: 6823–6833.
23 Rutledge EA, Halbert CL, Russell DW. Infectious clones and vectors derived from adeno-associated virus (AAV) serotypes other than AAV type 2. *J Virol* 1998; 72: 309–319.
24 Bantel-Schaal U, Delius H, Schmidt R, zur Hausen H. Human adeno-associated virus type 5 is only distantly related to other known primate helper-dependent parvoviruses. *J Virol* 1999; 73: 939–947.
25 Chiorini JA, Kim F, Yang L, Kotin RM. Cloning and characterization of adeno-associated virus type 5. *J Virol* 1999; 73: 1309–1319.
26 Xiao W *et al*. Gene therapy based on adeno-associated virus type 1. *J Virol* 1999; 73: 3994–4003.
27 Summerford C, Samulski RJ. Membrane-associated heparan sulfate proteoglycan is a receptor for adeno-associated virus type-2 virions. *J Virol* 1998; 72: 1438–1445.
28 Duan D *et al*. Enhancement of muscle delivery with pseudotypes adeno-associated virus type 5 correlates with myoblast differentiation. *J Virol* 2001; 75: 7662–7671.
29 Rabinowitz JE *et al*. Cross-packaging of a single adeno-associated virus (AAV) type 2 vector genome into multiple AAV serotypes enables transduction with broad specificity. *J Virol* 2002; 76: 791–801.
30 Walters RW *et al*. Binding of adeno-associated virus type 5 to 2,3-linked sialic acid is required for gene transfer. *J Biol Chem* 2001; 276: 20610–20616.
31 Sferra TJ *et al*. Recombinant adeno-associated virus-mediated correction of lysosomal storage within the central nervous system of the adult mucopolysaccharidosis Type VII mouse. *Hum Gene Ther* 2000; 11: 507–519.
32 Elliger SS, Elliger CA, Lang C, Watson GL. Enhanced secretion and uptake of β-glucuronidase improves adeno-associated viral-mediated gene therapy of mucopolysaccharidosis Type VII mice. *Mol Ther* 2002; 5: 617–626.
33 Frisella WA *et al*. Intracranial injection of recombinant adeno-associated virus improves cognitive function in a murine model of mucopolysaccharidosis Type VII. *Mol Ther* 2001; 3: 351–358.
34 Fu H *et al*. Neurological correction of lysosomal storage in a mucopolysaccharidosis IIIB mouse model by adeno-associated virus-mediated gene therapy. *Mol Ther* 2002; 5: 42–49.
35 Alisky JM *et al*. Tranduction of murine cerebellar neurons with recombinant FIV and AAV5 vectors. *Mol Neurosci* 2000; 11: 2669–2673.
36 Kaplitt MG *et al* . Long-term gene expression and phenotypic correction using adeno-associated virus vectors in the mammalian brain. *Nat Genet* 1994; 8: 148–154.
37 McCown TJ *et al*. Differential and persistent expression of CNS gene transfer by an adeno-associated virus (AAV) vector. *Brain Res* 1996; 713: 99–107.
38 During MJ *et al* . *In vivo* expression of therapeutic genes for dopamine production in the caudates of MPTP-treated monkeys using an AAV vector. *Gene Therapy* 1998; 5: 820–827.
39 Peel AL, Klein RL. Adeno-associated virus vectors: activity and applications in the CNS. *J Neurosci Methods* 2000; 98: 95–104.
40 Shimazaki K *et al*. Adeno-associated virus vector-mediated bcl-2 gene transfer into post-ischemic gerbil brain *in vivo*: prospects for gene therapy of ischemic-induced neuronal death. *Gene Therapy* 2000; 7: 1244–1249.
41 Mastakov MY, Baer K, Kotin RM, During MJ. Recombinant adeno-associated virus serotypes 2-and 5-mediated gene transfer in the mammalian brain: quantitative analysis of heparin co-infusion. *Mol Ther* 2002; 5: 371–380.
42 Passini MA, Lee EB, Heuer GG, Wolfe JH. Distribution of a lysosomal enzyme in the adult brain by axonal transport and by cells of the rostral migratory stream. *J Neurosci* 2002; 22: 6436–6446.
43 Bartlett JS, Samulski RJ, McCown TJ. Selective and rapid uptake of adeno-associated virus type 2 in brain. *Hum Gene Ther* 1998; 9: 1181–1186.
44 Hildinger M *et al*. Hybrid vectors based on adeno-associated virus serotypes 2 and 5 for muscle-directed gene transfer. *J Virol* 2001; 75: 6199–6203.
45 Heuer GG *et al*. Selective neurodegeneration in murine mucopolysaccharidosis VII is progressive and reversible. *Ann Neurol* 2002; 52: 762–770.
46 Barthel LK, Raymond PA. *In situ* hybridization studies of retinal neurons. *Methods Enzymol* 2000; 316: 579–590.

Zhu, J., et al. (2000) In-
se VI increases left ven-
n 102(19), 2396–2401.
nd Engler, R. L. (1989)
fusions of complement
e myocardial ischemia

16

Gene Delivery to the Mouse Brain with Adeno-Associated Virus

Marco A. Passini, Deborah J. Watson, and John H. Wolfe

1. Introduction

The efficient transduction of postmitotic cells by adeno-associated virus (AAV) makes it an excellent vector to deliver marker, functional, or therapeutic genes to the mammalian brain. An attractive feature of AAV is that all the viral-coding sequences are removed when engineering the recombinant genome, thereby limiting the extent of cell toxicity and immune response that are often associated with viral gene transcription *(1)*.

Of the seven described AAV serotypes, AAV serotype-2 (AAV2) is the most studied gene-transfer vehicle for in the mammalian brain. A feature of AAV2 transduction in the brain is that the vector remains confined to the injection site and predominately infects neurons rather than glia *(2–8)*. The limited diffusion of AAV2 vectors is beneficial for controlled gene delivery. For instance, targeting therapeutic genes only to brain structures showing pathology would eliminate complications associated with vector diffusion and subsequent expression in healthy structures, and is an important consideration when designing treatment strategies for localized neurodegenerative diseases. The same is true for other experimental paradigms, such as investigating the function of genes in specific brain structures or using marker genes in tract-tracing experiments. Although AAV2 vectors were shown to remain predominately at the injection site, one study demonstrated that the vector itself may undergo axonal transport in inter-regional systems *(9)*.

From: *Methods in Molecular Biology, vol. 246:*
Gene Delivery to Mammalian Cells: Vol. 2: Viral Gene Transfer Techniques
Edited by: W. C. Heiser © Humana Press Inc., Totowa, NJ

The seven AAV serotypes differ from one another by their capsid proteins *(10–14)*. The fundamental basis for viral infection involves the interaction between the capsid proteins with molecules on the surface of the host cell. Thus, the different AAV serotypes target different cell-surface receptors for binding, which may lead to complementary and unique transduction patterns in the central nervous system (CNS). This was illustrated by the finding that AAV2 and AAV5 use different attachment receptors on cell surfaces *(15–17)*, which explains the different transduction patterns observed for both serotypes in the brain *(7,18)* and retina *(19)*, as well as lung *(20)* and muscle *(21)*. Furthermore, AAV5 was shown to diffuse further through the mouse brain parenchyma compared to AAV2 *(7)*. Although the attachment receptors for the other AAV serotypes have not been identified, AAV4 shows a strong preference for transducing ependymal cells of the brain rather than the underlying parenchyma, and also transduces the retina very efficiently following subretinal injection into adult rats *(19)*. AAV1 and has yet to be examined in the brain, but has been shown to transduce the retina with moderate efficiency *(19)*.

Successful gene transfer to the CNS must also rely on activity from the promoter supporting expression. Previous reports demonstrated that the duration of AAV vector expression declined in the adult rodent brain when using viral promoters *(3,22–26)*. This could be owing to the inability of certain brain regions to support transcription following the methylation of viral regulatory sequences, as observed with the cytomegalovirus (CMV) promoter *(27)*. The downregulation of CMV was attenuated when the chicken β-actin enhancer was attached to CMV to produce a hybrid promoter *(5)*. When a pure mammalian regulatory promoter was engineered into an AAV genomic vector, such as the neuronal-specific enolase and platelet-derived growth factor promoters, long-term expression was observed in the CNS *(23–26,28)*. However, the relatively large size of both the pure or hybrid promoters is a disadvantage when engineering recombinant genomes owing to size limitations in AAV packaging reactions *(29)*. Our laboratory has used a small, eukaryotic housekeeping promoter (human β-glucuronidase) *(30,31)* capable of long-term expression in multiple brain structures *(8,32)*. The 378 base-pair human β-glucuronidase promoter would therefore provide a distinct advantage in somatic gene-transfer experiments involving large cDNAs.

Gene transfer with AAV2 to the developing brain has also been performed in newborn mice *(32–34)*. The smaller size of the neonatal brain is better suited for achieving global delivery of the transferred gene, because intraparenchymal injection of a volume of AAV2 would cover a larger area of the developing brain compared with a similar injected volume into an adult brain. Furthermore, intraventricular injection of AAV2 results in widespread brain transduction when the vector is administered into the cerebrospinal fluid (CSF) during neonatal devel-

opment *(32)*, whereas similar intraventricular injection into the adult brain results in a very limited transduction pattern *(7)*. In addition to achieving widespread gene delivery, administration of AAV2 vectors during neonatal development may provide a better clinical outcome for a wide variety of inherited CNS diseases by blocking the onset of pathology or by reducing the severity of the disease.

In this chapter, we describe how to deliver genes to the adult brain. Any AAV serotype can be used with this procedure. The protocol for neonatal gene delivery is found elsewhere and will not be covered in this chapter *(32–35)*. The information obtained in this chapter should aid in AAV-mediated somatic gene-transfer experiments to the adult mammalian brain.

2. Materials

2.1. AAV Vectors for Brain Injections

1. AAV virions generated by triple transfection *(36,37)* work well in gene-transfer experiments to the mammalian brain (*see* **Note 1**). Titers ranging from 10^{12}–10^{13} genomic particles/mL should be used to ensure high in vivo transduction efficiency.
2. Sterile, autoclaved glycerol should be added to the viral stock solution to a final concentration of 5%. Aliquots ranging from 20–50 µL should be made and frozen at −80°C to avoid multiple freeze-thaw cycles.
3. On the day of injection, remove tube(s) from −80°C and thaw on ice. Load the viral solution into the Hamilton syringe when ready to begin surgery.

2.2. Brain Surgery

1. Anesthesia. Ketamine (100 mg/mL, Ketaset, Fort Dodge Animal Health, Fort Dodge, Iowa) and Xylazine (20 mg/mL, Phoenix Pharmaceutical Inc., St. Joseph, MO), 0.9% sterile saline, disposable sterile syringes with 27 G needles (Fisher, Pittsburgh, PA).
2. Surgical Preparation. Small electric shaver and disposable scalpel (Webster Veterinary Supply, Sterling, MA), ethanol swabs (Fisher), stereotaxic frame (Kopf Small Animal Stereotaxic Frame Model 900, David Kopf Instruments, Tujunga, CA).
3. Drilling and Injection. Drill and drill bits (Foredom FM3545 control with MH145 hand-piece, Kopf), Hamilton syringe with 26–30 G needle for vector injections (Fisher), and pump (Stoeltling 310; Stoelting Co, Wood Dale, IL).
4. Manual. Manuals and review articles for stereotaxic surgery are helpful in illustrating the steps of surgery, and are available *(38,39)*.
5. Atlas. A mouse brain atlas will be helpful in determining the stereotaxic coordinates for the brain structures of interest *(40)*.

6. Postoperative care. Absorbable suture thread (Vicryl with C3 needle, Ethicon, Inc. Somerville, NJ) and heating pad (Gaymar Industries, Orchard Park, NY).

2.3. Transcardial Perfusion and Dissection of Brain from Skull

1. Perfusion. Dissecting tray, sterile 1X PBS, fixative (4% paraformaldehyde/1X PBS, pH, 7.4), large scissors for cutting the skin, fine scissors for cutting the abdominal wall and diaphragm, forceps, butterfly needle (23 × 3/4 in infusion set, Abbott Laboratories no. 4565, Chicago, IL), three-way valve, infusion pump, and tubing.
2. Dissection. Bone crusher (RS8282, Roboz Surgical Instrument Company, Inc., Rockville, MD).

2.4. Preparation of Brain Tissue for Cyrosectioning

1. 30% Sucrose, 100% optimal cutting temperature (OCT) solution (Sakura Finetek USA, Torrance, CA), disposable plastic molds (Polysciences, Inc., Warrington, PA), slides (Fisher).

2.5. Reagents for Detection of β-Glucuronidase on Frozen Tissue Sections

1. Solution 1 (Chloral hydrate formalin fixative): 1% chloral hydrate in 20% (v/v) neutral-buffered formalin in distilled water: Mix 0.1 g chloral hydrate (Sigma C8383, St. Louis, MO), 20 mL neutral-buffered formalin, 80 mL deionized water. Chloral hydrate is extremely hygroscopic. A DEA license is required for chloral hydrate purchase and use. Store at 4°C.
2. Solution 2: Chloral-formal-acetone fixative). Mix seven parts acetone to three parts solution 1.The solution will be cloudy when first mixed. Put at 37°C until clear, then filter through 0.45 μm filter. Store at 4°C.
3. Solution 3: 0.2 *M* sodium acetate buffer. Mix 20 mL of 1 *N* HCl, 40 mL of 1 *M* sodium acetate and 140 mL deionized water. Adjust pH to 4.5. Store at 4°C.
   a. Solution 3a: 0.05 *M* sodium acetate, pH 4.5. Dilute solution 3 at 1:4 with deionized water and adjust the pH to 4.5. Store at 4°C.
   b. Solution 3b: 0.05 *M* sodium acetate, pH 5.2. Dilute solution 3 at 1:4 with deionized water and adjust the pH to 5.2. Store at 4°C.
4. Solution 4 (0.25 m*M* napthol AS-BI β-D-glucuronide in 0.05 *M* sodium acetate buffer, pH 4.5): Add 13.7 mg napthol AS-BI β-D-glucuronide (Sigma N1875) to 100 mL of solution 3a. Dissolve with stirring at 37°C but do not raise the temperature above 50°C. Store at 4°C.
5. Solution 5: 0.25 m*M* napthol AS-BI β-D-glucuronide in 0.05 *M* sodium acetate buffer, pH 5.2. Add 13.7 mg napthol AS-BI β-D-glucuronide (Sigma

N1875) to 100 mL of solution 3b. Dissolve with stirring at 37°C but do not raise the temperature above 50°C. Store at 4°C.

6. Components of the substrate solution.
   a. Solution 6a (4% pararosaniline chloride). Dissolve 0.04 g pararosaniline chloride (Sigma P3750) in 1.0 mL 2 *N* HCl. Make 1 d before use and vortex well to mix. Store at 4°C for up to 3 wk.
   b. Solution 6b (4% sodium nitrite). Dissolve 0.04 g sodium nitrite (Fisher S347-250) in 1 mL deionized water. Make 1 d before use and vortex well to mix. Store at 4°C for up to 1 wk.
7. To make the filtered substrate solution (prepare 10–30 min before staining): Mix equal volumes of solution 6a and 6b (add the pararosaniline to the sodium nitrite to minimize precipitation). Add 1 volume of the mixture to 500 volumes of solution 5 (e.g., 20 µL of the 6a/6b mixture to 10 mL of solution 5). Filter through a 0.45-µm filter before use.
8. 1% aqueous methyl green extracted three to four times with $CHCl_3$.
9. Aqua Polymount (Polysciences, Inc.).

3. Methods

3.1. Brain Surgery

1. Weigh the adult mouse to determine the amount of anesthesia to inject into the intraperitoneal cavity (*see* **Note 2**). Use a dose of 100 mg/kg of ketamine and 5 mg/kg of Xylazine. When the mouse does not respond to pinching of the footpad, it is anesthetized.
2. Shave the head with an electric razor and swab the scalp with 70% ethanol. Make a straight incision along the midline of the head to expose the underlying skull.
3. Mount the mouse on a stereotaxic frame, and make sure that the head is level. Ear bars should also be used to fix the head in place to maintain proper 3-D alignment for the stereotaxic coordinates.
4. Align the drill directly over bregma. This morphological landmark is the intersection between the coronal and sagital suture lines. Using the coordinates of bregma as a reference point, move the drill using the anterior–posterior and medial–lateral knobs to the desired coordinates of the brain structure of interest.
5. Carefully move the skin to one side with a sterile cotton swab. Activate the drill and carefully lower it using the dorsal–ventral knob. As the drill touches the outside of the skull, carefully continue turning the knob so that the drill presses onto the skull with more pressure. Raise the drill on a consistent basis to determine if complete penetration of the skull occurred. Once the drill-hole is made, raise the drill and remove it from the stereo-

taxic frame and replace it with a Hamilton syringe that contains the AAV2 vector solution.

6. Lower the Hamilton syringe into the drill-hole so that the tip of the needle is approx 0.5 mm below the top base of the skull. Consider this location as the top of the pial surface of brain.
7. Lower the needle into the parenchyma to the desired depth (*see* Note 3). After reaching the target site, inject 1–2 µL of the AAV solution at a rate of 0.2 µL/min.
8. Once the injection is complete, leave the needle in place for 1–2 min to ensure complete absorption of the virus to the surrounding area. Then, raise the needle slowly to prevent back-flow of the virus out of the injection hole.
9. Remove the mouse from the stereotaxic frame and suture the scalp. Place the cage on a heating pad and cover the cage floor with a paper towel. Place the mouse on the paper towel and wet a small handful of food and place near the mouse. The mouse will lick the water off the food when it begins to recover from the surgery to prevent becoming dehydrated. The mouse should wake up from surgery after 30 min and be groggy in the cage between 1–4 h postoperation. Once the mouse is moving, place the cage back in the ventilated rack.

3.2. Transcardial Perfusion and Dissection of Brain from Skull

Transcardial perfusion results in fixation of molecules in the brain and overall maintenance of morphology.

1. Deeply anesthetize the mice with a dose of 0.1 mL of 5.0 mg of ketamine and 1.0 mg of xylazine.
2. Carefully make an incision along the belly of the mouse that extends to the top of the chest. Hold the abdominal wall with forceps and cut the wall with fine scissors. Do not cut the organs below.
3. When the ribcage is reached, cut the diaphragm on the left side to enter the chest cavity. Do not initially cut the right side of the diaphragm because you may puncture the heart.
4. The heart should be beating. Locate and cut the right atrium to allow for the blood to drain during the perfusion.
5. Holding the heart with forceps, locate the left ventricle and carefully insert a butterfly needle and perfuse with 1X PBS. Do not insert the needle too deep. The liver should turn light in color. Perfuse 10–15 mL of 1X PBS over a 5-min period.
6. After perfusing with 1X PBS, perfuse with approx 30–35 mL of fixative solution over a 20-min span (*see* **Note 4**). The perfusion should be done in the hood to avoid inhaling the fixative. Remove the needle when completed.

7. Cut the skin over the head and expose the skull. Using a bone crusher, make a small break at the back of the skull. This should expose the medulla. Carefully, work your away from the back of the brain to the front with the bone crushers. Forceps may be used to help remove the bone as you are moving around the skull. Remove the brain and place it in fresh fixative solution and incubate overnight at 4°C.

3.3. Preparation of Brain for Cyrosectioning

1. Transfer the brain to a fresh tube containing 30% sucrose at 4°C (*see* **Note 5**). The brain will initially float. Incubate the brain until it sinks, which takes approx 24–36 h.
2. Remove the sunken brain from the 30% sucrose solution and transfer it to a plastic mold containing 100% OCT. Let the brain infiltrate in the 100% OCT at room temperature for 1 h.
3. Make a flat bed of crushed dry-ice (−80°C) (*see* **Note 6**). In the plastic mold, stand the brain on the olfactory bulb for coronal, on its side for sagital, or flat for horizontal sections. The 100% OCT is very viscous and the brain will maintain its correct suspended position for a small time period before tipping over. Use forceps to help the brain maintain the desired orientation if it begins to tip.
4. Place the plastic mold on top of the dry-ice and keep monitoring the brain so that it doesn't tip before freezing in the block. Use forceps to guide it back into the proper orientation. After the block is completely frozen, transfer the block to −80°C for storage.
5. On the night before cyrosectioning, transfer the block to −20°C to equilibrate to the cutting temperature. Using a cryotome, cut sections ranging from 5–20 μm in thickness.
6. Slides designated for β-galactosidase or other enzyme staining reactions, or immuno-histochemistry should be stored at −20°C. Slides designated for *in situ* hybridization should be stored at −80°C. Protocols pertaining to the analysis of gene-transfer experiments to the brain for β-galactosidase ***(41)*** and β-glucuronidase ***(6,42)*** enzyme staining reactions, immunohistochemistry ***(3,22,23)***, and *in situ* hybridization ***(32,43,44)*** are available.

3.4. Analysis of β-Glucuronidase Expression on Frozen Tissue Sections

1. Bring the slides to room temperature (20 min) and draw a ring around the sections with a hydrophobic slide marker (such as PAP pen, Kiyota Intl. Inc).
2. Immerse the sections in solution 2 for 30 min at 4°C.
3. Wash the slides in three changes of solution 3a. It is essential to rehydrate the slides well. If the slides are in a rack, 3X 10 min incubations with agitation at 4°C will suffice.

4. Incubate the slides in solution 4 for 4 h to overnight at 4°C.
5. Remove the slides, aspirate the remaining fluid, and remark the hydrophobic well if necessary.
6. Place the slides horizontally in a flat tray and add the filtered substrate solution to cover the sections.
7. Incubate the trays horizontally overnight in a humidified 37°C incubator.
8. Stop the reaction by rinsing the slides well in distilled water. Counterstain with 1% methyl green if desired.
9. Cells positive for β-glucuronidase activity will be visualized by a red precipitate. For long-term storage, mount a coverslip with Aqua Polymount and store at room temperature.

4. Notes

1. DNA harvested by Qiagen (Valencia, CA) maxi-prep is suitable to be used in triple transfection protocols when generating recombinant AAV virions.
2. Inhalant anesthesia can be substituted for injectable anesthesia in fragile mice strains. In this case, a precision isoflurane vaporizor should be used at a range of 1.5–3.0% (SurgiVet Inc., Waukesha, WI).
3. If injections are to be done in multiple structures along the dorsoventral axis, inject the ventralmost structure first and then raise the needle dorsally to the subsequent site(s).
4. Improper perfusion will result in the brain being malleable to touch when dissecting the tissue from the skull. Improper perfusion may also contribute to a lacy brain, which can interfere with the analysis.
5. Another major contributor to a lacy brain is insufficient cryoprotection. If one were to freeze the brain before it has completely sunken in the 30% sucrose solution, the nondisplaced water molecules would form ice crystals during the freezing process. The formation of these ice crystals would produce holes in the brain.
6. Isopentane-liquid nitrogen can be substituted for dry ice during the freezing process *(40)*.

Acknowledgments

This work was supported by NIH grants DK46637, NS38690, and DK63973 (JHW), institutional NRSA training grants in gene therapy (DK 7748) (MAP) and neurovirology (NS07180) (DJW), and an individual NRSA postdoctoral Fellowship (NS 11024) (to DJW).

References

1. Xiao, X., Li, J., McCown, T. J., and Samulski, R. J. (1997) Gene transfer by adeno-associated virus vectors into the central nervous system. *Exp. Neurol.* **144**, 113–124.

ight at 4°C.
and remark the hydropho-

d the filtered substrate so-

midified 37°C incubator.
stilled water. Counterstain

e visualized by a red pre-
lip with Aqua Polymount

prep is suitable to be used
recombinant AAV virions.
able anesthesia in fragile
aporizor should be used at
VI).
es along the dorsoventral
1 raise the needle dorsally

malleable to touch when
usion may also contribute
ysis.
fficient cryoprotection. If
ely sunken in the 30% su-
; would form ice crystals
se ice crystals would pro-

dry ice during the freez-

3690, and DK63973 (JHW),
) (MAP) and neurovirology
Fellowship (NS 11024) (to

7) Gene transfer by adeno-
Exp. Neurol. **144,** 113–124.

2. Kaplitt, M. G., Leone, P., Samulski, R. J., Xiao, X., Pfaff, D. W., O'Malley, K. L., and During, M. J. (1994) Long-term gene expression and phenotypic correction using adeno-associated virus vectors in the mammalian brain. *Nat. Genet.* **8,** 148–154.
3. Chamberlin, N. L., Du, B., de Lacalle, S., and Saper, C. B. (1998) Recombinant adeno-associated virus vector: use for transgene expression and anterograde tract tracing in the CNS. *Brain Res.* **793,** 169–175.
4. Bartlett, J. S., Samulski, R. J., and McCown, T. J. (1998) Selective and rapid uptake of adeno-associated virus type 2 in brain. *Hum. Gene Ther.* **9,** 1181–1186.
5. Mandel, R. J., Rendahl, K. G., Spratt, S. K., Snyder, R. O., Cohen, L. K., and Leff, S. E. (1998) Characterization of intrastriatal recombinant adeno-associated virus-mediated gene transfer of human tyrosine hydroxylase and human GTP-cyclohydrolase I in a rat model of parkinson's disease. *J. Neurosci.* **18,** 4271–4284.
6. Skorupa, A. F., Fisher, K. J., Wilson, J. M., Parente, M. K., and Wolfe, J. H. (1999) Sustained production of β-glucuronidase from localized sites after AAV vector gene transfer results in widespread distribution of enzyme and reversal of lysosomal storage lesions in a large volume of brain in mucopolysaccharidosis VII mice. *Exp. Neurol.* **160,** 17–27.
7. Davidson, B. L., Stein, C. S., Heth, J. A., Martins, I., Kotin, R. M., Derksen, T. A., et al. (2000) Recombinant adeno-associated virus type 2, 4, and 5 vectors: transduction of variant cell types and regions in the mammalian central nervous system. *Proc. Natl. Acad. Sci. USA* **97,** 3428–3432.
8. Passini, M. A., Lee, E. B., Heuer, G. G., and Wolfe, J. H. (2002) Distribution of a lysosomal enzyme in the adult brain by axonal transport and by cells of the rostral migratory stream. *J. Neurosci.* **22,** 6437–6446.
9. Kaspar, B. K., Erickson, D., Schaffer, D., Hinh, L., Gage, F. H., and Peterson, D. A. (2002) Targeted retrograde gene delivery for neuronal protection. *Mol. Ther.* **5,** 50–56.
10. Chiorini, J. A., Yang, L., Liu, Y., Safer, B., and Kotin, R. M. (1997) Cloning of adeno-associated virus type-4 (AAV4) and generation of recombinant AAV4 particles. *J. Virol.* **71,** 6823–6833.
11. Cliorini, J. A., Kim, F., Yang, L., and Kotin, R. M. (1999) Cloning and characterizing of adeno-associated virus type-5. *J. Virol.* **73,** 1309–1319.
12. Rutledge, E. A., Halbert, C. L., and Russell, D. W. (1998) Infectious clones and vectors derived from adeno-associated virus (AAV) serotypes other than AAV type 2. *J. Virol.* **72,** 309–319.
13. Bantel-Schaal, U., Delius, H., Schmidt, R., and Van Hausen, H. (1999) Human adeno-associated virus type 5 is only distantly related to other known primate helper-dependent parvovirus. *J. Virol.* **73,** 939–947.
14. Xiao, W., Chirmule, N., Berta, S. C., McCullough, B., Gao, G. P., and Wilson, J. M. (1999) Gene therapy based on adeno-associated virus type 1. *J. Virol.* **73,** 3994–4003.
15. Summerford, C. and Samulski, R. J. (1998) Membrane-associated heparin sulfate proteoglycan is a receptor for adeno-associated virus type 2 virions. *J. Virol.* **72,** 1438–1445.

16. Bartlett, J. S., Wilcher, R., and Samulski, R. J. (2000) Infectious entry pathway of adeno-associated virus and adeno-associated virus vectors. *J. Virol.* **74,** 2777–2785.
17. Walters, R. W., Yi, S. M. P., Keshavjee, S., Brown, K. E., Welsh, M. J., Chiorini, J. A., and Zabner, J. (2001) Binding of adeno-associated virus type 5 to 2,3 sialic acid is required for gene transfer. *J. Biol. Chem.* **276,** 20610–20616.
18. Alisky, J. M., Hughes, S. M., Sauter, S. L., Jolly, D., Dubensky, T. W., Staber, P. D., et al. (2000) Transduction of murine cerebellar neurons with recombinant FIV and AAV5 vectors. *Neuroreport* **1,** 2669–2673.
19. Rabinowitz, J. E., Rolling, F., Li, C., Conrath, H., Xiao, W., Xiao, A., and Samulski, R. J. (2002) Cross-packaging of a single adeno-associated virus (AAV) type 2 vector genome into multiple AAV serotypes enables transduction with broad specificity. *J. Virol.* **76,** 791–801.
20. Zabner, J., Seiler, M., Walters, R., Kotin, R., Fulgeras, W., Davidson, B. L., and Chiorini, J. A. (2000) Adeno-associated virus type 5 (AAV5) but not AAV2 binds to the apical surface of airway epithelia and facilitates gene transfer. *J. Virol.* **74,** 3852–3858.
21. Duan, D., Yan, Z., Yue, Y., Ding, W., and Engelhardt, J. F. (2001) Enhancement of muscle gene delivery with pseudotyped adeno-associated virus type 5 correlates with myoblast differentiation. *J. Virol.* **75,** 7662–7671.
22. McCown, T. J., Xiao, X., Li, J., Breese, G. R., and Samulski, R. J. (1996) Differential and persistent expression patterns of CNS gene transfer by an adeno-associated virus (AAV) vector. *Brain Res.* **713,** 99–107.
23. Klein, R. L., Meyer, E. M., Peel, A. L., Zolotukhin, S., Meyers, C., Muzyczka, N., and King, M. A. (1998) Neuron-specific transduction in the rat septohippocampal or nigrostriatal pathway by recombinant adeno-associated virus vector. *Exp. Neurol.* **150,** 183–194.
24. Klein, R. L., Mandal, R. J., and Muzyczka, N. (2000) Adeno-associated virus vector-mediated gene transfer to somatic cells in the central nervous system. *Adv. Virus Res.* **55,** 507–528.
25. Peel, A. L. and Klein, R. L. (2000) Adeno-associated virus vectors: activity and applications in the CNS. *J. Neurosci. Meth.* **98,** 95–104.
26. Xu, R., Janson, C. G., Mastakov, M., Lawlor, P., Young, D., Mouravlev, A., et al. (2001) Quantitative comparison of expression with adeno-associated virus (AAV-2) brain-specific gene cassettes. *Gene Ther.* **8,** 1323–1332.
27. Prosch, S. J., Stein, K., Staak, C., Liebenthal, H., Volk, H. D., and Kruger, D. H. (1996) Inactivation of the very strong HCMV immediate early promoter by DNA CpG methylation *in vitro*. *Biol. Chem. Hoppe. Seyler* **377,** 195–201.
28. Peel, A. L., Zolotukhin, S., Schrimsher, G. W., Muzyczka, N., and Reier, P. J. (1997) Efficient transduction of green fluorescent protein in spinal cord neurons using adeno-associated virus vectors containing cell type-specific promoters. *Gene Ther.* **4,** 16–24.
29. Dong, J. Y., Fan, P. D., and Frizzell, R. A. (1996) Quantitative analysis of the packaging capacity of recombinant AAV. *Hum. Gene Ther.* **7,** 2101–2112.

30. Shipley, J. M., Miller, R. D., Wu, B. M., Grubb, J. H., Christensen, S. G., Kyle, J. W., and Sly, W. S. (1991) Analysis of the 5′ flanking region of the human β-glucuronidase gene. *Genomics* **10,** 1009–1018.
31. Wolfe, J. H., Kyle, J. W., Sands, M. S., Sly, W. S., Markowitz, D. G., and Parente, M. K. (1995) High level expression and export of β-glucuronidase from murine mucopolysaccharidosis VII cells corrected by a double-copy retrovirus vector. *Gene Ther.* **2,** 70–78.
32. Passini, M. A. and Wolfe, J. H. (2001) Widespread gene delivery and structure-specific patterns of expression in the brain from an adeno-associated virus vector following intraventricular injections of neonatal mice. *J. Virol.* **75,** 12382–12392.
33. Elliger, S., Elliger, C., Aguilar, C., Raju, N., and Watson, G. (1999) Elimination of lysosomal storage in brains of MPS VII mice treated with intrathecal administration of an adeno-associated virus vector. *Gene Ther.* **6,** 1175–1178.
34. Frisella, W. A., O'Connor, L. H., Vogler, C. A., Roberts, M., Walkley, S., Levy, B., et al. (2001) Intracranial injection of recombinant adeno-associated virus improves cognitive function in a murine model of mucopolysaccharidosis type VII. *Mol. Ther.* **3,** 351–358.
35. Snyder, E. Y., Taylor, R. M., and Wolfe, J. H. (1995) Neural progenitor cell engraftment corrects lysosomal storage throughout the MPS VII mouse brain. *Nature* **374,** 367–370.
36. Fisher, K. J., Jooss, K., Alston, J., Yang, Y., Haecker, S. E., High, K., et al. (1997) Recombinant adeno-associated virus for muscle-directed gene therapy. *Nature Med.* **3,** 306–312.
37. Gao, G. P., Wilson, J. M., and Wivel, N. A. (2000) Production of recombinant adeno-associated virus. *Adv. Virus Res.* **55,** 529–543.
38. Cooley, R. K. and Vanderwold, C. H. (1990) *Stereotaxic Surgery in the Rat: a Photographic Series*. A.J. Kirby Co., London, Ontario.
39. Brooks, A. I., Halterman, M., Chadwick, C., Davidson, B., Haak-Frendscho, M., Radel, C., et al. (1998) Reproducible and efficient murine CNS gene delivery using a microprocessor-controlled injection. *J. Neurosci. Methods* **80,** 137–147.
40. Franklin, K. B. J. and Paxinos, G. (1997) *The Mouse Brain: in Stereotaxic Coordinates*. Academic Press, CA.
41. Watson, D. J., Kobinger, G. P., Passini, M. A., Wilson, J. M., and Wolfe, J. H. (2002) Transduction patterns in the mouse central nervous system by lentivirus vectors pseudotyped with envelope proteins from vesicular stomatitis virus, ebola virus, mikola virus, lymphocytic choriomeningitis virus, or murine leukemia virus. *Mol. Ther.* **5,** 528–537.
42. Wolfe, J. H. and Sands, M. S. (1996) Murine mucopolysaccharidosis type VII: a model for somatic gene therapy of the central nervous system, in *Protocols for Gene Transfer in Neuroscience: Towards Gene Therapy of Neurological Disorders* (Lowenstein, P. R. and Enquist, L.W., eds.) John Wiley & Sons Ltd., London, pp. 263–274.

43. Passini, M. A., Levine, E. M., Canger, A. K., Raymond, P. A., and Schechter, N. (1997) Vsx-1 and Vsx-2: differential expression of two paired-like homeobox genes during zebrafish and goldfish retinogenesis. *J. Comp. Neurol.* **388,** 495–505
44. Barthel, L. K. and Raymond, P. A. (2000) *In situ* hybridization studies of retinal neurons. *Methods Enzymol.* **316,** 579–590.